Science of the Total Environment 662 (2019) 110–120

Contents lists available at ScienceDirect

Science of the Total Environment

journal homepage: www.elsevier.com/locate/scitotenv

Preferential meltwater flowpaths as a driver of preferential elution of chemicals from melting snowpacks

Diogo Costa[a, b, *], John W. Pomeroy[a, b]

[a] Centre for Hydrology, University of Saskatchewan, Canada
[b] Global Institute for Water Security, University of Saskatchewan, Canada

HIGHLIGHTS

- Nutrient release from melting snowpacks affects biogeochemical cycling in cold regions
- Preferential flowpaths (PFP) in melting snowpacks and rain-on-snow impact the snowpack discharge process
- High-frequency flow and chemistry measurements were used to investigate the elution of snow ions during early snowmelt
- PFP released and transported more that 20% of the total NO_3 and PO_4 snowpack load during the first 1.5% of snowmelt
- Climate change is expected to increase the frequency of ROS events which may reduce the magnitude of this early ionic pulse

GRAPHICAL ABSTRACT

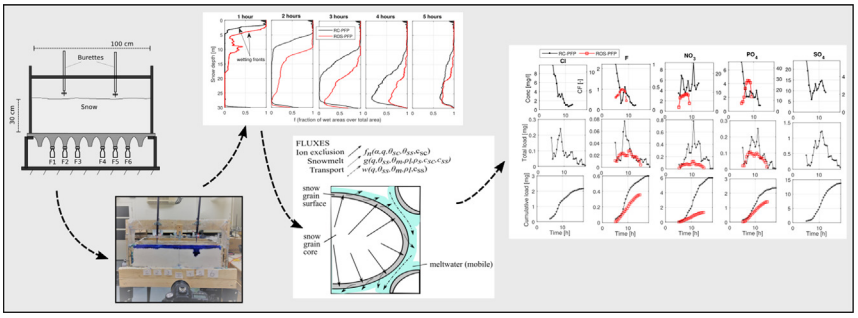

ARTICLE INFO

Article history:
Received 7 November 2018
Received in revised form 8 January 2019
Accepted 9 January 2019
Available online 21 January 2019

Editor: Xinbin Feng

ABSTRACT

Seasonal snowcovers release nutrients accumulated over the winter during spring snowmelt and this can be an important part of the annual biogeochemical cycling of chemicals and their loading to soils and water bodies. The characteristics of this load are controlled by snowmelt dynamics and the physical and chemical properties of the snowpack, which are affected by overwinter and snowmelt metamorphism, refreezing of meltwater, and ion exclusion from snow crystals. Rain-on-snow (ROS) events can accelerate and modify the snowpack discharge process. The interplay of these processes can cause microscale flow heterogeneity and preferential flow pathways (PFP). Previous experimental work has examined PFP and ion elution processes in snowpacks, but their combined effect on the spatial and temporal characteristics of snowmelt ion elution remains uncertain. In this research, two controlled laboratory experiments were performed to investigate the role of PFP and ROS in controlling snow ion release to runoff. These involved the high frequency monitoring of flow and meltwater concentrations during snowmelt induced by radiation-convection (RC) processes and rain-on-snow (ROS). Results showed that when ROS was included, PFP was responsible for

* Corresponding author at: Centre for Hydrology and Global Institute for Water Security, University of Saskatchewan, Canada
E-mail address: diogo.costa@arch.usask.ca (D. Costa).

https://doi.org/10.1016/j.scitotenv.2019.01.091
0048-9697/© 2019 Published by Elsevier B.V.

Keywords:
Snow hydrochemistry
Cold regions hydrology
Nutrient exports
Ion exclusion
Ion preferential elution
Acid snow

the transport of 68% and 73% of the total NO_3 and PO_4 load discharged during the early snowmelt phase recorded by the experiment. However, this initial load increased to 95% and 75% when ROS was removed, causing the release of more than 20% of the total snowpack NO_3 and PO_4 during the first 1.5% of melt. Small intensity ROS may refreeze in the snowpack, which may affect the ability of lateral flow to deliver snow ions located beyond the leading edge of PFP.

© 2019 Published by Elsevier B.V.

1. Introduction

Climate change is particularly affecting cold regions where warmer, shorter winters and increasing variability in precipitation are already causing changes in hydrology (e.g., Choi et al., 2010; Donat et al., 2013; Williams et al., 2015; Vincent et al., 2015; DeBeer et al., 2016; Rasouli et al., 2018). For instance, the frequency of rain-on-snow (ROS) events is expected to increase by 50% with a temperature rise of up to 2–4 $^{\circ}C$ before decreasing thereafter (Beniston and Stoffel, 2016; Morán-Tejeda et al., 2016). Simultaneously, nutrient fluxes from agricultural lands have been implicated in the increasing eutrophication of large northern lakes such as Lake Winnipeg and Lake Erie (e.g., Scavia et al., 2014), which are considered among the major freshwater crises in North America. In many cold regions, such as the Canadian Prairies, snowmelt runoff has a strong impact on nutrient export (e.g., Brooks et al., 1999; Brooks and Williams, 1999; Eimers et al., 2009; Casson et al., 2012), contributing with most of the phosphorous (P) and nitrogen (N) exported yearly (Corriveau et al., 2013). In this context, accurate model predictions of heterogeneous snowmelt and the associated nutrient export are important to inform nutrient management strategies in current and future climate and development scenarios (e.g. Costa et al., 2017; Arheimer et al., 2012; Harrington and Bales, 1998; Stein et al., 1986). However, these processes are poorly understood and often ignored in models (e.g., Costa et al., 2017, 2018).

Chemicals accumulate in the seasonal snowpack over the winter and are rapidly released via preferential elution during the spring snowmelt (Davies et al., 1987; Pomeroy et al., 2005). This can result in high chemical loading to soils (e.g., Lilbaek, 2007) and water bodies during this period (Jones, 1987; Tranter et al., 1987). The chemical load can lead to temporary acidification of streams and cause stress conditions for the aquatic biota including fish mortality (e.g., Driscoll et al., 1980; Gunn and Keller, 1984), particularly in cases where the soil has low buffering capacity (Wigington et al., 1990; Tranter et al., 1988) or the contact between meltwater and the soil matrix is limited by frost (Ferrier et al., 1989).

The release of chemicals from snowpacks during melt is a complex process with multiple spatial and temporal scales. The early components of meltwater eluent can carry 50–80 % of the total snowpack ion load in the first 1/3 of the meltwater volume (Brimblecombe et al., 1986; Maulé and Stein, 1990). The enhancement of initial concentrations is influenced by ion exclusion during ice crystal growth (Colbeck, 1981; Hewitt et al., 1991; Marsh and Pomeroy, 1999) which is caused by differences in the hydrated radii of ions and on the ability of ions to form hydrogen bonds (e.g., Na and Cl are incorporated more readily into the ice crystal lattice than NO_3 and SO_4) (Davies et al., 1987). This causes the formation of quasi-liquid layers on the surface of snow grains, the preferential enrichment of these layers with some ions (e.g., Colbeck, 1981; Hewitt et al., 1991; Marsh and Pomeroy, 1999) and their mixing with percolating meltwater. Other factors observed to affect the magnitude of early ionic pulses include the melt rate (Tranter, 1991; Davis et al., 1995), snow depth (Davies et al., 1987) freeze-thaw cycles (Colbeck, 1981; Davis et al., 1995) and distribution of ions within the snowpack (Bales et al., 1989; Pomeroy et al., 1993; Marsh and Pomeroy, 1999).

The melt rate is controlled by the snow surface energy balance which varies with space and time in response to meteorological conditions, slope and aspect (Pomeroy et al., 2003, 2016a). Snowmelt discharge rates and concentration distributions are affected by winter and snowmelt microscale changes in the internal physical and chemical properties of snow. The effect of melt rate on the release of ions from the snowpack has been examined by Davis et al. (1995) through a series of controlled laboratory experiments. They observed that slow melt rates caused higher ionic pulses when compared to rapid melt rates. It has been hypothesized that low melt rates are more efficient at removing chemicals from the snowpack due to two possible reasons: (1) more time for solute diffusion from the immobile ion-enriched quasi-liquid layers surrounding the snow grains to the meltwater front or finger, and (2) they cause more uniform melt and synchronous solute release from the entire snowpack, as opposed to higher flow rates where PF often develops.

Negative relationships between melt rates and concentration factors (CF) (i.e., ratio between meltwater concentration peaks and the average pre-melt snowpack concentration) have been observed across different geographical locations. Marsh and Pomeroy (1999) took daily observations of the major anions and cations in meltwater collected from a multi-compartment lysimeter installed into a snow pit wall in Trail Valley Creek, Canada, and observed that higher flow rates associated with preferential flow pathways (PFP) showed lower concentrations when compared to lower flow rates associated with matrix flow, which points to the conditions for meltwater ion enrichment hypothesized by Davis et al. (1995). Similarly, Tonnessen (1991) recorded a CF value for NO_3 of 6 for a 125-day long melt event in 1987 at Emerald Lake watershed, in Sierra Nevada, California (Harrington and Bales, 1998), while measurements in the spring of 1991 at different locations at Trail Valley Creek tundra basin, north of Inuvik, Canada (Pomeroy et al., 1993), showed higher CF values for NO_3 (approx. 8) for shorter melt rates - melt period ranged between 13.4 and 36 days depending on the sampling location (Marsh and Pomeroy, 1996, 1999). Observations at different locations at Trail Valley Creek showed a high spatial variability in snowmelt runoff chemistry, but similar CF values were obtained despite differences in the melt rate and snow depth (0.450 –1.850 m). While the formation of basal ice is known to greatly enrich meltwater ion-concentrations (Lilbæk and Pomeroy, 2008), and could explain some of these differences, little is understood about the effects of PFP on snow ion elution, which can be formed through radiation-convection (RC) or rain-on-snow (ROS) processes.

The effect of PFP in melting snowcovers has been observed in experiments using dye traces (Gerdel, 1954; Marsh and Woo, 1984a), but its influence on ion release by the percolating meltwater, as hypothesized by Davis et al. (1995), has not yet been examined. PFP are caused by flow instabilities at the leading edge of the wetting

front (e.g., Parlange, 1974). They are formed when the water-entry pressure (i.e., threshold value that allows water to enter a dry pore) is reached through a water ponding process on a less permeable layer boundary (Wakahama, 1963; Katsushima et al., 2013; Leroux and Pomeroy, 2017). Two conditions have been observed for the formation of water ponding layers (Katsushima et al., 2013): (1) a capillary barrier, i.e. fine-textured layer overlaying a coarse-textured layer (Wakahama, 1963; Jordan, 1995) and (2) a hydraulic conductivity barrier, i.e. an impermeable ice layer under a snow layer (Langham, 1974). As the PFP grows it readily mixes at the advancing position with ions situated on the surface of snow grains (Jury et al., 2003; Wang et al., 2004; Shiozawa and Fujimaki, 2004). Lateral flow from the surrounding snow matrix may also occur due to lower capillary pressure along horizontal interfaces between snow layers or where ice layers develop (Cho et al., 2005; Selker et al., 1992; Katsushima et al., 2013). The suction of lateral flow to the PFP entry points can promote PFP growth (Jury et al., 2003; Wang et al., 2004; Shiozawa and Fujimaki, 2004), and extend the contact area between meltwater and ion-enriched snow layers to other regions of the snow matrix beyond the PFP entry points.

PFP in melting snowpacks develop naturally through RC processes, but can be strongly affected by ROS events. In RC-induced melt, PFP form due to microscale heterogeneities in the pore-size distribution causing spatial differences in water-entry pressure, which promotes the formation of microscale flow structures. ROS events form when rain falls on a pre-existing snowpack (Marks et al., 1998; Beniston and Stoffel, 2016; Pomeroy et al., 2016b), causing rapid rainwater-snow energy transfers that can accelerate snowmelt and metamorphism, and promote vertical PFP at the rain entry points (Avanzi et al., 2013). Besides being a flood hazard (e.g., Hilker et al., 2009; Rössler et al., 2014; Beniston and Stoffel, 2016) because they can cause the quick melt of large volumes of snow, studies have shown that ROS events can also cause early, rapid mobilization of snow and soil N and P (e.g. Galloway et al., 1987; Tranter, 1991; Jones, 1999; Mitchell, 2001; Groffman et al., 2001). Eimers et al. (2007), for instance, analyzed a forested catchment in south-central Ontario and found that in-stream NO_3 concentrations increased rapidly after ROS events and accounted for up to 40% of the total annual export. Casson et al. (2010) compared 18 other catchments with different physiographic characteristics within the same region and observed a similar patter - median export of NO_3 − N from ROS events of 55%. In turn, Miles et al. (2013) monitored an agricultural catchment in Ontario, the Beaver River sub-watershed of Lake Simcoe, and found that a single ROS event could also mobilize most of the dissolved phosphorous (DP) exported annually, and Ball Coelho et al. (2012) investigated other catchments in the same region and found similar results, with 28% of the dissolved and organic P being exported during a single ROS event.

Following on the theoretical considerations advanced by Davis et al. (1995), it is hypothesized that snow structures and PFP flow have a strong impact on the spatial-temporal dynamics of nutrient release because they determine the total snow grain surface area accessible for mixing with percolating meltwater. The research presented in this paper focuses on the impact of PFP formed during radiation-convection driven snowmelt at microscale-induced flow structures and ROS-induced PFP formed from surface depressions on the mechanisms of snowpack solute release in melting snowpacks. Ion removal efficiencies are examined through controlled laboratory experiments where PFP are formed both from the radiation-convection at the snow surface and through the additional action of ROS to advect energy through liquid water application to the snow surface. The research aims to better understand the snowpack hydrology processes governing ion elution. This is an essential step to better understanding the role of snowmelt in contributing to nutrient exports in cold regions and improving hydrochemistry model predictions.

2. Materials and methods

2.1. Experimental set-up

Fig. 1 shows the experiment setup in the hydrochemistry laboratory of the Centre for Hydrology, University of Saskatchewan. It consists of an insulated box with holes at the base expanding vertically into funnels (assembled from a commercial seed tray) and connected to sampling bottles. Expanded polystyrene plates were used as insulation. The box was subdivided into three disconnected

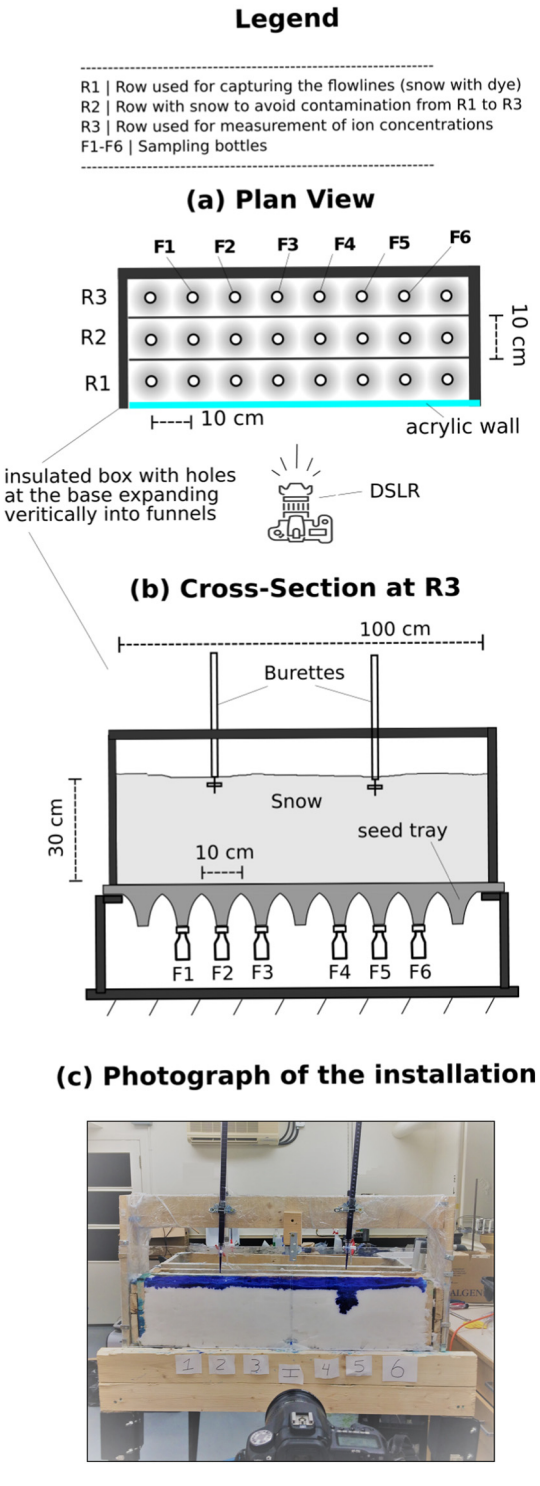

Fig. 1. Schematic views of the experiment setup.

areas, rows R1–R3, each containing equal number of holes and funnels. Row R1 was used to monitor the wetting front and PFP using commercial ink and a DSLR camera. The dividing wall to the exterior was replaced by an acrylic wall for this purpose. Row 3 was used to monitor snowmelt discharge volumes and concentrations. Burettes were placed directly above funnels F2 and F5 to simulate ROS. Row 2 served as an additional row of snow between R1 and R3 (panel a, Fig. 1) to avoid contamination of the snow in R3 by the ink used to trace the wetting front in R1. The holes and funnels along row R3 were connected to sampling bottles (panel b, Fig. 1). Lines were drawn on the bottles at a level corresponding to a 18.4 ml sample, a volume that was considered both sufficient for posterior laboratory analysis and adequate for capturing the temporal dynamics of meltwater concentrations. All components of the installation were PET, HDPE or wrapped in plastic film prior to the start of the experiment.

2.2. Experimental protocol

The snow used in this experiment was collected in March of 2017 from an agricultural field near the Town of Clavet, 20 km east of Saskatoon, Saskatchewan, Canada. New PET bags and a clean scoop wrapped in a triple layer of PET plastic were used to avoid contamination. At the time of collection, the air temperature was approximately −6°C, and the snow was composed mostly by rounded crystals. The time of collection is important because in Saskatchewan snowpacks are seasonal and tend to be matured by spring when the major annual snowmelt event (and the associated nutrient export) occurs. The collection point was remote from major sources of roadway or other surface contamination, but some increase in Cl levels was expected from road salt from a nearby highway. The snow was brought to a temperature-controlled cryospheric environmental laboratory located in the Centre for Hydrology, University of Saskatchewan, and stored at a constant temperature of −22°C. The room contains a dual refrigerating system (Heatcraft, BZ series) with stable cooling capacity from +7.5 to −30°C(± 2 °C) and is sealed to prevent contamination of samples from dust and air particulates.

The snow was carefully handled in the cryospheric lab at −20°C during the preparation of the experiment. This was to reduce snow metamorphism from temperature gradients and minimize the risk of contamination. Firstly, the snow was thoroughly mixed to guarantee homogeneous snow properties (e.g., density and ion concentrations). This was performed using clean plastic scoops prior to the snow being transferred to the experimental box while it was still in the sampling bags. Samples were taken to measure snow density and the average ion concentration of the parent snow, which were used to calculate the total snow mass and snow-water-equivalent (SWE) as well as the total mass of ions (see Table 1). Secondly, the experimental box was filled with snow to a height of 30 cm without any compaction to avoid unevenly affecting the porosity distribution, which could impact the formation of PFP. The snow depth chosen was considered a good compromising between the practicality of the experiment and the order of magnitude found in many cold regions, such the Canadian Prairies. Thirdly, a thin layer of snow mixed with dye was added to the top of the snow column in row R1. The snow in row R3, where the meltwater samples were collected, was covered during this operation to minimize the risk of contamination.

Two experiments were performed, one where PFP were left to occur from melt driven by radiation and convection (RC) in a room warmed to 19 °C(RC-PFP), and one at the same room temperature where additional PFP were induced through water applied at the snow surface to simulate ROS (ROS-PFP). In the ROS-PFP experiment, water was applied from the two burettes along the R1 row (for PFP observation) which were filled with snow mixed with dye, while the two burettes along the R3 row (for snowmelt chemistry analysis) were filled with snow only. The snow used to fill the burettes was the same used to prepare the snowpack and was allowed to melt at the temperature of the room (19 °C). All the components of the experimental set-up were thoroughly cleaned and rinsed with deionized water (milliQ) prior to the experiment. Several blanks were taken to ensure no background contamination.

On the day of the experiment, the installation was moved from the cryospheric environment laboratory to the hydrochemistry laboratory which had an average temperature of 19 °C. Photographs of cross-sectional area of the snowpack were taken at 15-minute intervals with a DSLR camera, and the MATLAB Image Processing Toolbox was used to estimate the fraction of wet (with blue dye) to the total cross-sectional area. The meltwater collected in the sampling bottles was filtered using syringe filters of 0.5 µm pore size, and frozen for posterior laboratory analysis. The samples were tested for major anions (chloride (Cl), fluoride (F), nitrate (NO_3), phosphate (PO_4) and sulfate (SO_4)), using a DIONEX Ion Chromatography system and an AS-AP autosampler.

The estimated duration of snowmelt was about 30 h. However, the experimental protocol involved a detailed and continuous sampling procedure that could only be maintained during the first 20 h(approx. 66% of the total melt). This was considered a good compromise between the practicability of conducting such fine-scale (temporal and spatial) sampling, and the focus of the experiment on the initial phase of melt where nutrients are known to be exported in larger quantities - previous observations of preferential elution of snowpacks have shown that the initial 1/3 of meltwater carried 50–80 % of the total snow ion mass (e.g., Marsh and Pomeroy, 1999).

Table 1
Measured properties of the snow: density, ionic concentrations and total snow and ionic masses. The total mass of snow was calculated by multiplying the average density of the snow (500 kg/m^3) by the volume of snow added: dimensions of the experimental box (10×100cm) times the snow depth (30 cm). The total mass of ions was calculated by multiplying the average snow ionic concentrations ("Value" column) by the estimated SWE computed from the total mass of snow.

Property	Value	Total Mass
Density	500 ± 20 kg/m^3	15 ± 0.6 kg of snow$^{\&}$
Cl	0.8307 ± 0.4591 mg/l	12.46 ± 6.8865 mg
F	bdl	n.a.
NO_3	0.3621 ± 0.4272 mg/l	5.43 ± 6.87 mg
PO_4	0.1564* mg/l	2.35 mg
SO_4	4.5504 ± 3.3425 mg/l	68.25 ± 50.14 mg

bdl: below the detection limit
$^{\&}$0.03 m^3 of snow; 15 litres of snow-water-equivalent (SWE)
* only one sample was above the detection limit

3. Results

3.1. Spatial Heterogeneity

3.1.1. The Ripening phase and Preferential flow

Fig. 2 shows the fraction of wet to total cross-sectional area (f) during the warming and ripening phases, which had a similar duration of about 5 h in both experiments. Direct observation of the images showed that the RC-PFP experiment had warming and ripening phases of approximately 1 and 4 h, respectively. In the case of the ROS-PFP experiment, the added water at the air-snow interface forced the warming and ripening phases to synchronize with a combined duration of approximately 5 h. The wetting front resulting from the combined effect of both PFP and matrix flow advanced more rapidly in the ROS-PFP experiment (compare the RC-PFP and ROS-PFP cases throughout the experiment in Fig. 2), but the f profiles of both snowpacks merged at the end of the ripening phase (5-hours panel). This was probably because the input flux (ROS) only occurred at two locations (2 burettes) and at relatively low flow rates (Fig. 1 in Supplementary Material), which may have caused the water to enter the snowpack and refreeze shortly after. Such fixed drip zones

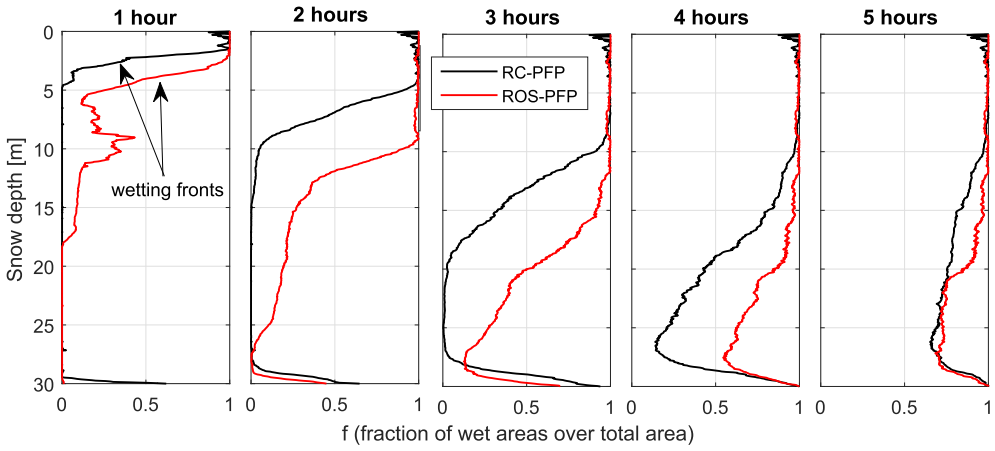

Fig. 2. Snowpack profiles of the fraction of wet areas over total cross-sectional area (*f*) during the ripening phase for both the RC-PFP (black line) and ROS-PFP (red line) experiments.

can occur naturally as drip lines under forest canopies. The wetting fronts in both snowpacks became more diffuse after 2 h into the melting process due to the advancement of the PFP fronts and their detachment from the main bulk wetting front.

Fig. 3 shows the cumulative discharge observed at each sampling location (F1–F6) for both the RC-PFP and ROS-PFP experiments. Two distinct flow rates can be observed, which correspond to locations that intercepted the PFP at the bottom of the snowpack (red lines) and those that received matrix flow (black lines). As expected, the locations with PFP did not coincide between the two experiments. This is because the direction and speed of the leading edge of the flow fingers depend on the spatial distribution of water-entry capillary pressure which is affected by small, local changes in the pore distribution. However, in the case of the ROS-PFP experiment, the positioning of the burettes (directly above F2 and F5) resulted in the formation of PFP above those locations (lines F2 (ROS) and F5 (ROS)). In the RC-PFP experiment, location F4 observed a significant increase in the flow rate (line F4 (RC)) after 10 h into the experiment (and 5 h after the start of the output phase). This was probably due to microscale changes in the snow structure, permeability and lateral flow causing the merging of flow channels and/or connection to water pockets that had been retained inside the snowpack. During the first 13 h of the experiment, the locations connected to PFP discharge points (red lines) accumulated twice as much water as did those only receiving matrix flow (black lines).

3.1.2. Dynamics of snow ion release (time-space)

Fig. 4 shows the ion load (a) and concentrations (b) of meltwater measured at the different discharge locations. Results in Fig. 5a reveal that snowmelt ion loads and concentrations are highly variable both temporally (x-axis) and spatially (different lines), particularly in the RC-PFP experiment (black line) The variability observed at local scales is caused by the combined effect of microscale flow and ionic concentration heterogeneities within the snow column.

The results show that PFP water (red lines, Fig. 5a) is responsible for a higher portion of the total load for most ions. During the time of the experiment (approximately 16 h), PF flow transported the following fractions of the total ion load: 69% for Cl, 50% for F, 95% for NO_3, 75% for PO_4, and 55% for SO4, for the RC-PFP experiment, and 71% for F, 68% for NO_3, and 73% for PO_4, for the ROS-PFP experiment. The total load exported during RC-induced snowmelt was generally higher than that induced by ROS. This may be because ROS

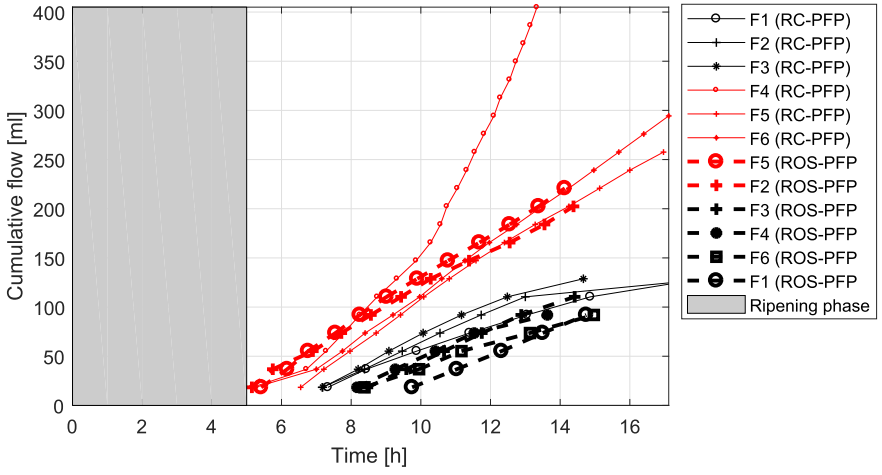

Fig. 3. Cumulative discharge measured at each sampling location (F1–F6) for both experiments: RC-PFP (thin lines) and ROS-PFP (thick lines). The red and black colors are used to distinguish between the locations connected to PFP discharge points from those only receiving matrix flow, respectively.

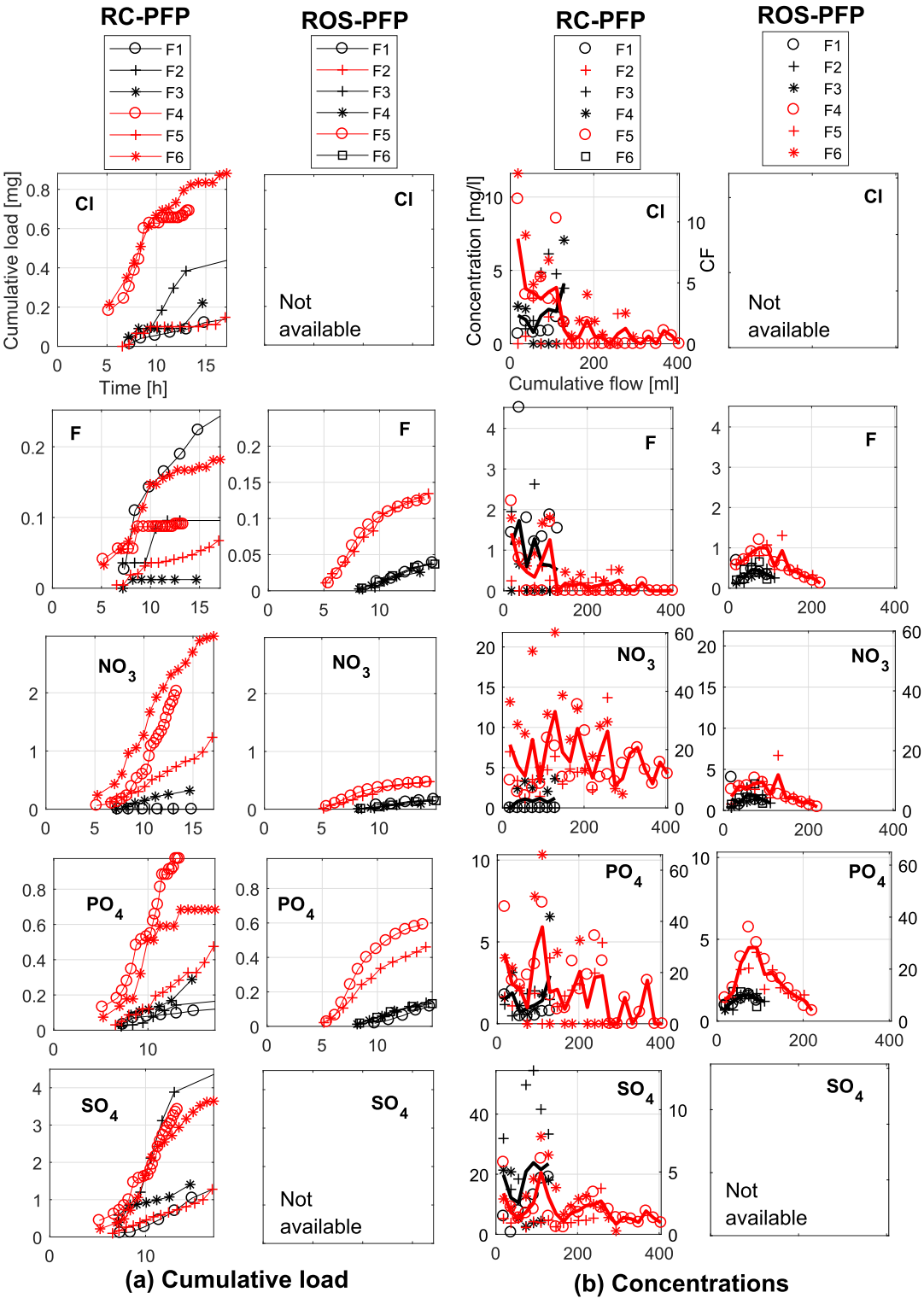

Fig. 4. Cumulative ionic load (a) and meltwater concentrations (b) measured for both the RC-PFP (left column of plots in panels a and b) and ROS-PFP (right column of plots in a and b) experiments. The ionic loads (a) are plotted as a function of the time elapsed since the start of the warming phase (beginning of the experiment), while the meltwater concentrations (b) are plotted against the cumulative flow. The locations connected to PFP discharge points are represented with red markers and the locations receiving matrix flow with black markers, with the solid lines representing the calculated arithmetic mean.

forces PFP vertically at specific entry points before the snowpack has reached isothermal conditions at 0 °C(warming phase) and melt and wet metamorphism has been initiated. This may lead to poor lateral hydraulic connections between the PFP (flow channel) advancing location and adjacent regions, as opposed to RC-induced snowmelt that overall promotes more hydraulically connected microscale flow channels. The meltwater concentration peaks are also generally higher for the regions receiving PFP (red lines, Fig. 5b), suggesting

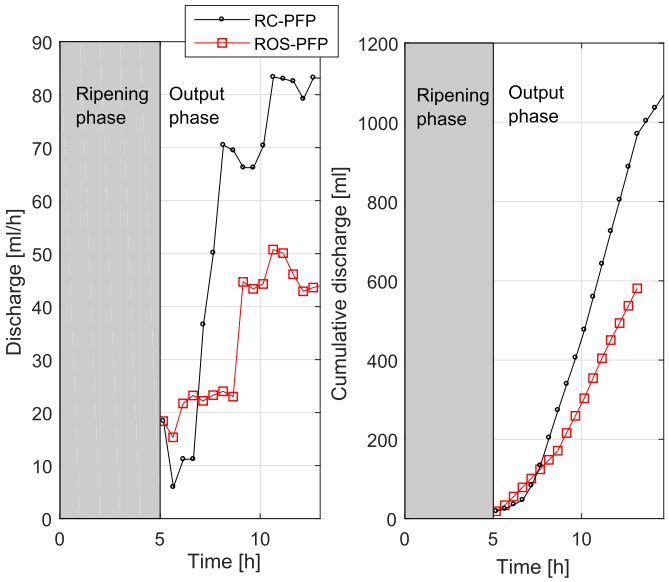

Fig. 5. Snowpack discharge rate (left) and cumulative discharge volume (right) measured for both the RC-PFP and the ROS-PFP experiments.

that the higher loads transported by preferential flow are not only caused by higher flows but also due to higher concentrations (i.e., higher release of snow ions).

3.2. The effect of PF and ROS on the overall snowpack response

Fig. 5 shows the hourly discharge rate and cumulative discharge volume calculated from sum of the interval discharge volumes measured in all bottles. The output phase was characterized by an initial rapid increase in the discharge rate until steady-state conditions established. The unsteady flow phase had a duration of approximately 2 h in both experiments. The discharge rate and total discharge volumes were 2 times higher for the RC-PFP experiment than for the ROS-PFP one. The difference in the total cumulative flow between the two experiments becomes apparent after 2 h through the experiment is related to the timing when the different sampling bottles started receiving water, with only 2 bottles in the RC-PFP experiment against 6 in the ROS-PFP one during the first 8 h through the experiment (see Fig. 3). It should be noted that in this experiment the ROS event was simulated through two localized water input fluxes of varying intensity (see Fig. 1 in Supplementary Material) to capture its particular effect on PFP, but the added water was temporarily held in the pore space through tension forces and probably refrozen from heat transfer with the snow matrix. This formed ice lenses that would have decreased the porosity and conductivity of the snowpack, temporary reducing and delaying meltwater discharge.

Fig. 6 summarizes the main patterns observed in the two experiments: the estimated concentrations (left axis) and CFs (right axis) in the upper graphs, the total ionic loads (middle graphs), and cumulative total ionic loads (lower graphs) in meltwater discharge for the different ions. These ion concentrations and loads were calculated from the sum of sample volumes and concentrations measured from all sampling bottles. As expected, early ionic pulses are observed for most chemical species (upper graphs), and are followed by a gradual decrease in concentrations. NO_3 unexpectedly showed a concentration increase throughout the experiments. The maximum CF factors (right-y axis) varied significantly depending on the ion, which is indicative of fractionation as well as preferential ion elution, as observed in previous studies (e.g. Tranter et al., 1987). The ions CFs can be ordered in the following sequence: $PO_4 > NO_3 > Cl > SO_4 > F$. This sequence is similar for both experiments, although the highest CF values were observed for the RC-PFP experiment.

A similar pattern to that observed for concentrations can be found for ion loads (middle plots), which is marked by a rapid increase in the load during the early stages of melt. This was expected given the

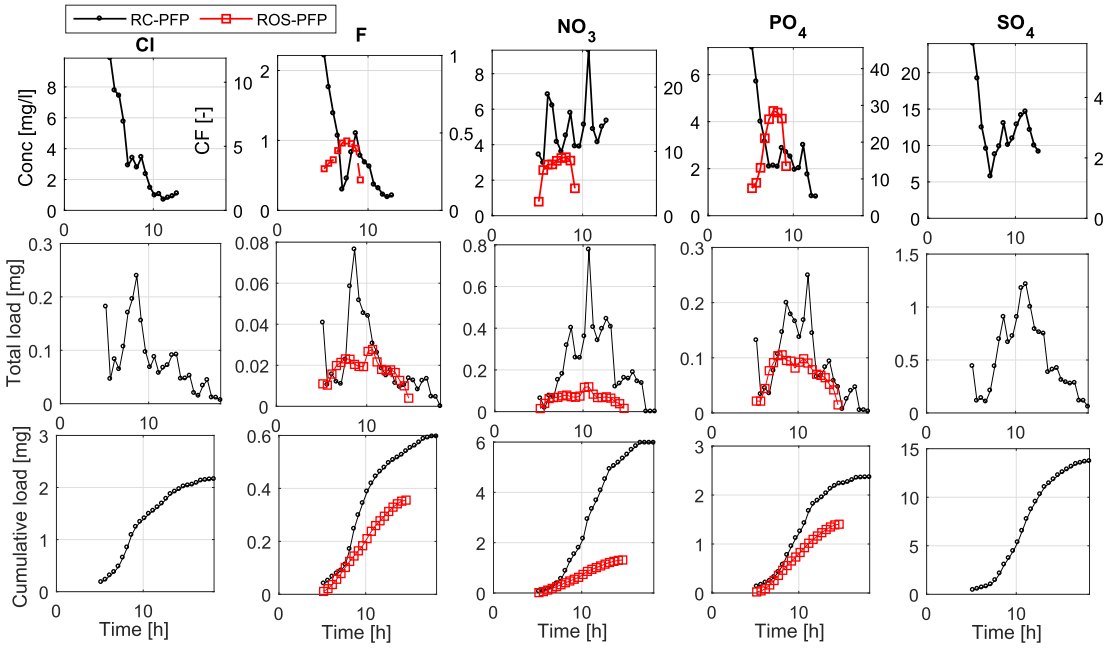

Fig. 6. Average meltwater concentrations (left axis) and CFs (right axis) in the upper panels, total snowpack discharge load in the middle panels and cumulative load in the lower panels. Results are presented for the different ions and for both experiments: RC-PFP (black lines), and ROS-PFP (red lines). Since CFs are essentially the ratio between meltwater concentrations (y-left axis) and the respective average pre-melt snowpack concentration (which is a constant), all lines throughout the different panels can be read from both y-left and y-right axis, except when the y-right axis is removed because snow concentrations were unavailable.

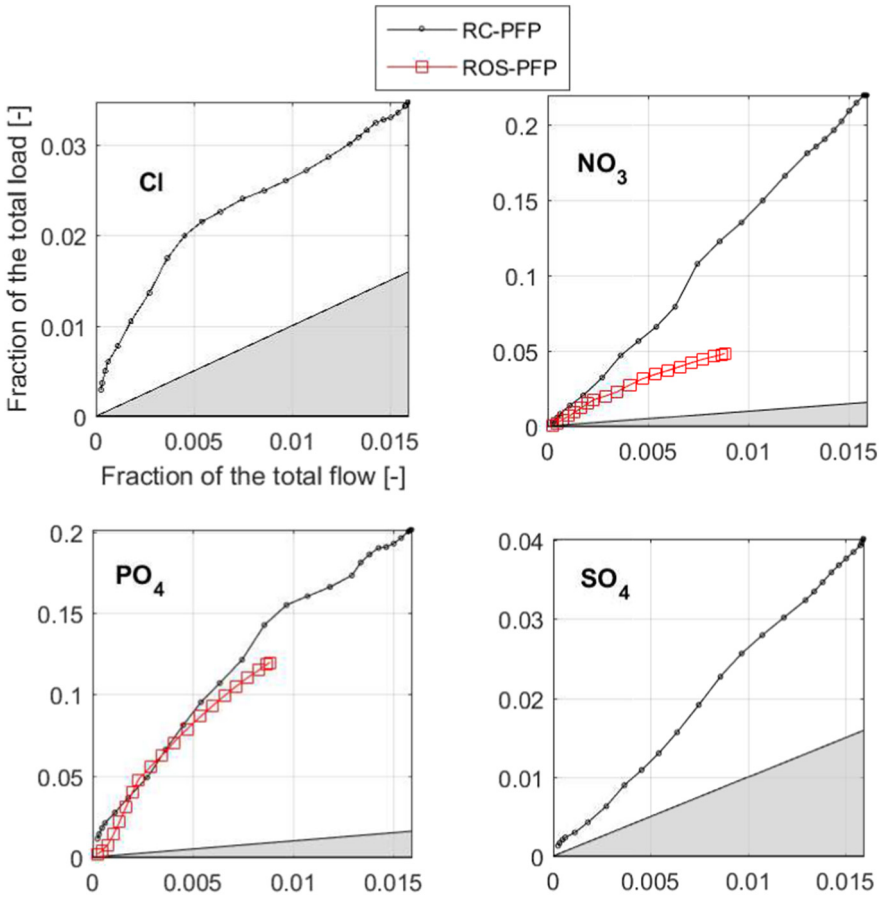

Fig. 7. Fraction of the cumulative ion load as a function of the fraction of the cumulative ion discharge. Lines above the grey area mean a ratio of total load to the total flow above one.

rapid development of steady-state discharge conditions (see Fig. 5), which caused the concentration dynamics to be the dominant control of the total load. A major fraction of the load was transported during the first 15 h into the experiment, or within 10 h of the start of snowpack meltwater discharge.

Fig. 7 shows the fraction of the total load transported as a function of the fraction of the total discharge. Both maximum total discharge and load were estimated using the properties observed in the parent snow (see Table 1; snow F concentrations were all below the detection limit). Similarly to Fig. 4, the results in Fig. 7 show that for most ions in both experiments, a higher fraction of the total load was eluted during the early stages of melt. The initial 1.5% of melt eluted as much as 3.5% of Cl, 25% of NO_3, 20% of PO_4, and 4% of SO4 snow load, in the parent RC-PFP case, and 5% of NO_3 and 12% of PO_4 of the snow load in the ROS-PFP case.

4. Discussion

4.1. Combined mechanisms of preferential flow and snow ion exclusion

Spatial and temporal variations in microscale snowmelt discharge, as observed in Figs. 2 and 3, are caused by heterogeneities in the internal microstructural properties of snow during snowmelt (e.g., Leroux and Pomeroy, 2017; Avanzi et al., 2013; Waldner et al., 2004). The physics of PFP generation and flow in melting snowcovers is relatively well documented (e.g., Gerdel, 1954; Marsh and Woo, 1984b). Tracer dyes have been commonly used in these studies to investigate snowpack meltwater percolation throughout the melting process and, similarly to our study, image processing techniques were often used to estimate the wet fractional cross-sectional area as a proxy for water content (e.g., Avanzi et al., 2013). As for meltwater chemistry, Marsh and Pomeroy (1993, 1999) provided a deeper look into the spatial variability of meltwater concentrations in natural snowcovers in the Arctic. They did not address the effect of ROS conditions as these did not occur during their monitoring program. Although spatial variability in meltwater concentrations has been observed, and similar methods have been used to assess the microhydrology of melt, these have not been combined to determine how PFP could be the driver of spatial variability in meltwater chemistry.

Microscale flow heterogeneity (PFP) caused high temporal and spatial variabilities in meltwater concentrations in both conditions of RC- and ROS-induced PFP development (Fig. 4). Concentration peaks in meltwater generally occurred earlier and were higher at the discharge locations receiving PFP water, which suggests that the higher ionic loads delivered by PFP were not only due to high flow rates, but also caused by higher concentrations. Flow fingers are caused by flow instabilities at the leading edge of the wetting front (e.g. Parlange, 1974). They are formed when the water-entry capillary pressure is reached through water ponding on a less permeable layer boundary (Wakahama, 1963; Katsushima et al., 2013; Leroux and Pomeroy, 2017).

The results of this experiment suggest that lateral flow redistribution towards PFP significantly enhances the transport of ions. Lateral flow towards the vertically advancing PFPs occurs due to higher capillary pressure at the advancing location when compared to the adjacent positions (Cho et al., 2005; Selker et al., 1992; Katsushima et al., 2013). This causes conditions for PFP growth (Jury et al., 2003; Wang et al., 2004; Shiozawa and Fujimaki, 2004),

which increases the opportunity time and contact area for mixing of meltwater with the ions that accumulate in quasi-liquid layers at the surface of snow grains due to over-winter snow ion exclusion (e.g., Colbeck, 1981; Hewitt et al., 1991; Pomeroy et al., 1993; Marsh and Pomeroy, 1999). This is hypothesized based on the evidence that the total load exported during this period was generally higher for the RC-PFP experiment, which as previously discussed, may have more permeable and well connected microscale flow structures during early melt, as opposed to the ROS-PFP case where the PFP were induced by depressions and the specific locations where the input water has entered the snow surface.

These results suggest that conditions promoting unstable flow and PFP in melting snowpacks are likely to intensify the early ionic pulses in snowmelt runoff. The susceptibility of porous materials, such as snowpacks, to form PFP increases with air entrapment, suction head or water-entry pressure, and soil layering and heterogeneity (e.g. Wang et al., 1998; Leroux and Pomeroy, 2017). However, it remains unclear whether climate change may favour conditions to PFP in melting snowpacks because the expected rise in air temperature will enhance snow metamorphism, which may reduce air entrapment and water-entry pressures, but may also increase soil layering and heterogeneity (e.g., formation of ice lenses) due to an increase in the frequency of freeze-thaw events.

4.2. Implications of RC-PFP and ROS-PFP to the overall snowpack response

The snowpack discharge rates and concentrations presented in Figs. 6 and 7 display the response patterns typically observed during snowmelt, e.g., Johannessen and Henriksen (1978), Waldner et al. (2004), Marsh and Woo (1984b) (for flow) and Marsh and Pomeroy (1999), Davis et al. (1995)) (for concentrations). The results show ionic pulses in meltwater discharge during the early phases of melt, a phenomenon that occurs primarily due to snow ion exclusion occurring during over-winter ice crystal growth (Jones, 1987; Tranter et al., 1987). Internal flow structures were observed in the snowpacks of the two experiments, but were particularly noticeable during the ripening phase and the beginning of the output phase.

Previous observations of preferential elution of snowpacks have shown that the initial 1/3 of meltwater carried 50–80 % of the total snow ion mass (Brimblecombe et al., 1986; Marsh and Pomeroy, 1999). This is caused by ion-enriched quasi-liquid layers forming at the surface of snow grains (Colbeck, 1981; Hewitt et al., 1991; Marsh and Pomeroy, 1999) and their mixing with snowmelt water as it percolates downwards into the snowpack. The results of this experiment show that the preferential elution process may be even more pronounced than previously thought, particularly in the seldom-observed very early stages of snowmelt. Here up to 25% of snow NO_3 and 20% of snow PO_4 were released during the first 1.5% of melt when snowmelt was induced by radiation-convection processes (RC-PFP experiment), as opposed to only 5% and 12% when ROS was present, respectively (Fig. 7). This ionic load was discharged during the first 10 h of melt, and the combination of snow ion exclusion processes with the type of mechanism inducing PFP were determinant to the intensity of early nutrient export (see Section 3.2). Thus, this research suggests that early nutrient export from melting snowpacks is not only controlled by snow ion exclusion processes as previously thought, but it also strongly depends on how well laterally connected the microscale flow channels are during those initial snowmelt phases (RC-PFP more than ROS-PFP) to enable the lateral transport of snowpack ions to PFP.

A previous study at the Central Sierra Snow Laboratory, California, focused on the effect of ROS on solute transport through snowpack using earth rare elements (Taylor et al., 1998; Feng et al., 2001). They induced artificial rainstorms on snowpacks using sprinklers with tap water. This contrasts with smaller and more localized water inputs using burettes and melted snow water in our experiment for specifically examining the roles of PFP in ion movement. However, they also found that snow tracers quickly moved through the snowpack during these events and that meltwater concentrations were positively related to the input rain flux.

Climate change is expected to increase the frequency of ROS events (Beniston and Stoffel, 2016; Morán-Tejeda et al., 2016), which based on our study suggests that the magnitude of early ionic pulses and loads in snowmelt discharge may be expected to decrease. However, more ROS events will mean that snowmelt runoff events will become more frequent, alongside with the associate ionic pulses, which may lead to important changes on annual nutrient flux patterns that may have ecosystems-level effects.

5. Conclusions

Predicting changes in nutrient export from melting snowpacks under climate change conditions requires a better understanding of the internal transport mechanisms that cause the ion pulses typically observed in snowmelt discharge and the timing of these pulses. In this study, the effect of PFP on the time-space characteristics of the snowmelt ionic load and concentrations was examined through two experiments involving the monitoring of melting snowpacks developing PFP via both RC processes and ROS. Results show that the locations at the bottom of the snowpack intercepting PFP transported 68–75%, 73–75 %, and 55% of the total NO_3, PO_4 and SO_4 load (PFP + matrix flow) discharged during the experiments. Similarly to previous studies, snow ion exclusion processes caused early ionic pulses in meltwater for all ions, and concentration-factors (CF) as high as 40 could be observed in both RC- and ROS-induced melt experiments. High CFs are partially due to the exceptionally high temporal resolution of the measurements and to early observations of eluent. PFP induced by RC processes generally showed higher concentration factors than ROS-induced PFP. It is hypothesized that PFPs forming from snowmelt without rain are more efficient at removing snow ions because they are a product of the formation of microscale flow structures from snowmelt metamorphism. This promotes greater opportunity time and permeability between flowpaths and liquid water pockets, as opposed to when PFPs are forced at particular locations by depressions and fixed water inputs at the surface.

Results also showed that up to 25% and 20% of the total NO_3 and PO_4 snow load was eluted in the first 1.5% of meltwater volume in the RC-PFP case, which in these experiments was discharged during the first 10 h of snowmelt. This suggests that the ion exclusion process may be even more pronounced than previously reported, and that this process combined with PFP are the dominant mechanisms controlling the quality of meltwater.

Acknowledgments

The authors would like to thank the Global Water Futures Programme, the Canada Excellence Research Chair in Water Security, the Canada Research Chair in Water Resources and Climate Change, the Canadian Water Network and the Natural Sciences and Engineering Research Council (NSERC) through its CREATE in Water Security and Discovery grants programs for financial support. A special thanks to Professor Steve Siciliano for providing access to his lab for processing the water samples. We thank also the lab technicians, Dr. Donkuru McDonald, Curtis Senger and Alix Schebel, as well as the student assistants Keenan Brockman and Uswah Aziz for their help with the experiments and lab analyses.

Appendix A. Supplementary data

Supplementary data to this article can be found online at https://doi.org/10.1016/j.scitotenv.2019.01.091.

References

Arheimer, B., Dahné, J., Donnelly, C., Lindström, G., Strömqvist, J., 2012. Water and nutrient simulations using the HYPE model for Sweden vs. the Baltic Sea basin - influence of input-data quality and scale. Hydrol. Res. 43, 315–329. https://doi.org/10.2166/nh.2012.010.

Avanzi, F., Hirashima, H., Yamaguchi, S., Katsushima, T., De Michele, C., 2013. Observations of capillary barriers and preferential flow in layered snow during cold laboratory experiments. Cryosphere 10, https://doi.org/10.5194/tc-10-2013-2016.

Bales, R.C., Davis, R.E., Stanley, D.A., 1989. Ion elution through shallow homogeneous snow. Water Resour. Res. 25, 1869–1877. https://doi.org/10.1029/WR025i008p01869.

Ball Coelho, B., Murray, R., Lapen, D., Topp, E., Bruin, A., 2012. Phosphorus and sediment loading to surface waters from liquid swine manure application under different drainage and tillage practices. Agric. Water Manag. 104, 51–61. https://doi.org/10.1016/j.agwat.2011.10.020.

Beniston, M., Stoffel, M., 2016. Rain-on-snow events, floods and climate change in the Alps: events may increase with warming up to 4 °C and decrease thereafter. Sci. Total Environ. 571, 228–236. https://doi.org/10.1016/J.SCITOTENV.2016.07.146.

Brimblecombe, P., Tranter, M., Tsiouris, S., Davies, T.D., Vincent, C.E., 1986. The chemical evolution of snow and meltwater. IAHS Publ. 155, 283–295.

Brooks, P.D., Campbell, D.H., Tonnessen, K.A., Heuer, K., 1999. Natural variability in N export from headwater catchments: snow cover controls on ecosystem N retention. Hydrol. Process. 13, 2191–2201. https://doi.org/10.1002/(SICI)1099-1085(199910)13:14/15<2191::AID-HYP849>3.0.CO;2-L.

Brooks, P.D., Williams, M.W., 1999. Snowpack controls on nitrogen cycling and export in seasonally snow-covered catchments. Hydrol. Process. 13, 2177–2190.

Casson, N.J., Eimers, M.C., Buttle, J.M., 2010. The contribution of rain-on-snow events to nitrate export in the forested landscape of south-central Ontario, Canada. Hydrol. Process. 24 (14). https://doi.org/10.1002/hyp.7692. n/a–n/a.

Casson, N.J., Eimers, M.C., Watmough, S.A., 2012. Impact of winter warming on the timing of nutrient export from forested catchments. Hydrol. Process. 26, 2546–2554. https://doi.org/10.1002/hyp.8461.

Cho, H., de Rooij, G.H., Inoue, M., 2005. The pressure head regime in the induction zone during unstable nonponding infiltration. Vadose Zone J. 4, 908. https://doi.org/10.2136/vzj2004.0158.

Choi, G., Robinson, D.A., Kang, S., Choi, G., Robinson, D.A., Kang, S., 2010. Changing northern hemisphere snow seasons. J. Clim. 23, 5305–5310. https://doi.org/10.1175/2010JCLI3644.1.

Colbeck, S., 1981. A simulation of the enrichment of atmospheric pollutants in snow cover runoff. Water Resour. Res. 17, 1383–1388.

Corriveau, J., Chambers, P.A., Culp, J.M., 2013. Seasonal variation in nutrient export along streams in the northern great plains. Water Air Soil Pollut. 224, 1594. https://doi.org/10.1007/s11270-013-1594-1.

Costa, D., Pomeroy, J., Wheater, H., 2018. A numerical model for the simulation of snowpack solute dynamics to capture runoff ionic pulses during snowmelt: the PULSE model. Adv. Water Resour. 122, 37–48. https://doi.org/10.1016/j.advwatres.2018.09.008.

Costa, D., Roste, J., Pomeroy, J., Baulch, H., Elliott, J., Wheater, H., Westbrook, C., 2017. A modelling framework to simulate field-scale nitrate response and transport during snowmelt: the WINTRA model. Hydrol. Process. 31, 4250–4268.

Davies, T.D., Brimblecombe, P., Tranter, M., Tsiouris, S., Vincent, C.E., Abrahams, P., Blackwood, I.L., 1987. The removal of soluble ions from melting snowpacks. In: Jones, H.G., Orville-Thomas, W.J. (Eds.), Seasonal Snowcovers: Physics, Chemistry, Hydrology. NATO ASI Series (Series C: Mathematical and Physical Sciences) Springer Netherlands, Dordrecht, pp. 337–392. https://doi.org/10.1007/978-94-009-3947-9_20.

Davis, R.E., Petersen, C.E., Bales, R.C., 1995. Ion flux through a shallow snowpack: effects of initial conditions and melt sequences. IAHS Publications-Series of Proceedings and Reports-Intern Assoc Hydrological Sciences. Wallingford [Oxfordshire]: IAHS, 1981-., pp. 115–128.

DeBeer, C.M., Wheater, H.S., Carey, S.K., Chun, K.P., 2016. Recent climatic, cryospheric, and hydrological changes over the interior of western Canada: a review and synthesis. Hydrol. Earth Syst. Sci. 20, 1573–1598. https://doi.org/10.5194/hess-20-1573-2016.

Donat, M.G., Alexander, L.V., Yang, H., Durre, I., Vose, R., Dunn, R.J., Willett, K.M., Aguilar, E., Brunet, M., Caesar, J., Hewitson, B., Jack, C., Klein Tank, A.M., Kruger, A.C., Marengo, J., Peterson, T.C., Renom, M., Oria Rojas, C., Rusticucci, M., Salinger, J., Elrayah, A.S., Sekele, S.S., Srivastava, A.K., Trewin, B., Villarroel, C., Vincent, L.A., Zhai, P., Zhang, X., Kitching, S., 2013. Updated analyses of temperature and precipitation extreme indices since the beginning of the twentieth century: the HadEX2 dataset. J. Geophys. Res. Atmos. 118, 2098–2118. https://doi.org/10.1002/jgrd.50150.

Driscoll, C.T., Baker, J.P., Bisogni, J.J., Jr., Schofield, C.L., 1980. Effect of aluminium speciation on fish in dilute acidified waters. Nature 284, 161–164. https://doi.org/10.1038/284161a0.

Eimers, M.C., Buttle, J.M., Watmough, S.A., 2007. The contribution of rain-on-snow events to annual NO3-N export from a forested catchment in south-central Ontario, Canada. Appl. Geochem. 22, 1105–1110. https://doi.org/10.1016/j.apgeochem.2007.03.046.

Eimers, M.C., Watmough, S.A., Paterson, A.M., Dillon, P.J., Yao, H., 2009. Long-term declines in phosphorus export from forested catchments in south-central Ontario. Can. J. Fish. Aquat. Sci. 1682–1692. https://doi.org/10.1139/F09-101.

Feng, X., Kirchner, J.W., Renshaw, C.E., Osterhuber, R.S., Klaue, B., Taylor, S., 2001. A study of solute transport mechanisms using rare earth element tracers and artificial rainstorms on snow. Water Resour. Res. 37, 1425–1435. https://doi.org/10.1029/2000WR900376.

Ferrier, R.C., Anderson, J.S., Miller, J.D., Christophersen, N., 1989. Changes in soil and stream hydrochemistry during periods of spring snowmelt at a pristine site in mid-Norway. Water Air Soil Pollut. 44, 321–337. https://doi.org/10.1007/BF00279262.

Galloway, J.N., Hendrey, G.R., Schofield, C.L., Peters, N.E., Johannes, A.H., 1987. Processes and causes of lake acidification during spring snowmelt in the West-Central Adirondack Mountains, New York. Can. J. Fish. Aquat. Sci. 44, 1595–1602. https://doi.org/10.1139/f87-193.

Gerdel, R.W., 1954. The transmission of water through snow. Eos Trans. AGU 35, 475–485. https://doi.org/10.1029/TR035i003p00475.

Groffman, P.M., Driscoll, C.D.T., Fahey, T.J., Hardy, J.P., Fitzhugh, R.D., Tierney, G.L., Henry, K.S., Welman, T. a., Demers, J.D., Nolan, S., 2001. Effects of mild winter freezing on soil nitrogen and carbon dynamics in a northern hardwood forest. Biogeochemistry 56, 191–213. https://doi.org/10.1023/A:1013024603959.

Gunn, J.M., Keller, W., 1984. Spawning site water chemistry and lake trout (Salvelinus namaycush) sac fry survival during spring snowmelt. Can. J. Fish. Aquat. Sci. 41, 319–329. https://doi.org/10.1139/f84-036.

Harrington, R., Bales, R., 1998. Modeling ionic solute transport in melting snow. Water Resour. Res. 34, 1727–1736. https://doi.org/10.1029/98WR00557.

Hewitt, A.D., Cragin, J.H., Colbeck, S.C., 1991. Effects of crystal metamorphosis on the elution of chemical species from snow. 48th Annual Eastern Snow Conference, Guelph, Ontario, Canada. pp. 1–10.

Hilker, N., Badoux, A., Hegg, C., 2009. The Swiss flood and landslide damage database 1972–2007. Technical Report.

Johannessen, M., Henriksen, A., 1978. Chemistry of snow meltwater: changes in concentration during melting. Water Resour. Res. 14, 615–619. https://doi.org/10.1029/WR014i004p00615.

Jones, H.G., 1987. Chemical dynamics of snowcover and snowmelt in a boreal forest. Seasonal Snowcovers: Physics, Chemistry, Hydrology. Springer Netherlands, Dordrecht, pp. 531–574. https://doi.org/10.1007/978-94-009-3947-9_24.

Jones, H.G., 1999. The ecology of snow-covered systems: a brief overview of nutrient cycling and life in the cold. Hydrol. Process. 13, 2135–2147. https://doi.org/10.1002/(SICI)1099-1085(199910)13:14/15<2135::AID-HYP862>3.0.CO;2-Y.

Jordan, R., 1995. Effects of capillary discontinuities on water flow retention in layered snow covers. Def. Sci. J. 45, 79–91.

Jury, W., Wang, Z., Tuli, A., 2003. A conceptual model of unstable flow in unsaturated soil during redistribution. Vadose Zone J. 2, 61–67. https://doi.org/10.2113/2.1.61.

Katsushima, T., Yamaguchi, S., Kumakura, T., Sato, A., 2013. Experimental analysis of preferential flow in dry snowpack. Cold Reg. Sci. Technol. 85, 206–216. https://doi.org/10.1016/j.coldregions.2012.09.012.

Langham, E.J., 1974. Phase equilibria of veins in polycrystalline ice. Can. J. Earth Sci. 11, 1280–1287. https://doi.org/10.1139/e74-120.

Leroux, N.R., Pomeroy, J.W., 2017. Modelling capillary hysteresis effects on preferential flow through melting and cold layered snowpacks. Adv. Water Resour. 107, 250–264. https://doi.org/10.1016/j.advwatres.2017.06.024.

Lilbaek, G., 2007. Compositional Change of Meltwater Infiltrating Frozen Ground.Ph.D. thesis. University of Saskatchewan.

Lilbæk, G., Pomeroy, J.W., 2008. Ion enrichment of snowmelt runoff water caused by basal ice formation. Hydrol. Process. 22, 2758–2766. https://doi.org/10.1002/hyp.7028.

Marks, D., Kimball, J., Tingey, D., Link, T., 1998. The sensitivity of snowmelt processes to climate conditions and forest cover during rain-on-snow: a case study of the 1996 Pacific Northwest flood. Hydrol. Process. 12, 1569–1587. https://doi.org/10.1002/(SICI)1099-1085(199808/09)12:10/11<1569::AID-HYP682>3.0.CO;2-L.

Marsh, P., Pomeroy, J.W., 1993. The impact of heterogeneous flow paths on snowmelt runoff chemistry. 50th Eastern snow conference. pp. 231..

Marsh, P., Pomeroy, J.W., 1996. Meltwater fluxes at an Arctic forest-tundra site. Hydrol. Process. 10, 1383–1400. https://doi.org/10.1002/(SICI)1099-1085(199610)10:10<1383::AID-HYP468>3.0.CO;2-W.

Marsh, P., Pomeroy, J.W., 1999. Spatial and temporal variations in snowmelt runoff chemistry, Northwest Territories, Canada. Water Resour. Res. 35, 1559–1567. https://doi.org/10.1029/1998WR900109.

Marsh, P., Woo, M.-K., 1984a. Wetting front advance and freezing of meltwater within a snow cover: 1. Observations in the Canadian Arctic. Water Resour. Res. 20, 1853–1864. https://doi.org/10.1029/WR020i012p01853.

Marsh, P., Woo, M.-K., 1984b. Wetting front advance and freezing of meltwater within a snow cover: 1. Observations in the Canadian Arctic. Water Resour. Res. 20, 1853–1864. https://doi.org/10.1029/WR020i012p01853.

Maulé, C.P., Stein, J., 1990. Hydrologic flow path definition and partitioning of spring meltwater. Water Resour. Res. 26, 2959–2970. https://doi.org/10.1029/WR026i012p02959.

Miles, J.J., Eimers, M.C., North, R.L., Dillon, P.J., 2013. Spatial distribution and temporal variability in the forms of phosphorus in the Beaver River subwatershed of Lake Simcoe, Ontario, Canada. Inland Waters 3, 179–186. https://doi.org/10.5268/IW-3.2.531.

Mitchell, M.J., 2001. Linkages of nitrate losses in watersheds to hydrological processes. Hydrol. Process. 15, 3305–3307. https://doi.org/10.1002/hyp.503.
Morán-Tejeda, E., López-Moreno, J., Stoffel, M., Beniston, M., 2016. Rain-on-snow events in Switzerland: recent observations and projections for the 21st century. Clim. Res. 71, 111–125. https://doi.org/10.3354/cr01435.
Parlange, J.-Y., 1974. Water movement in soils. Geophys. Surv. 1, 357–387. https://doi.org/10.1007/BF01449119.
Pomeroy, J.W., Essery, R.L.H., Helgason, W.D., 2016a. Aerodynamic and radiative controls on the snow surface temperature. J. Hydrometeorol. 17, 2175–2189. https://doi.org/10.1175/JHM-D-15-0226.1.
Pomeroy, J.W., Fang, X., Marks, D.G., 2016b. The cold rain-on-snow event of June 2013 in the Canadian Rockies - characteristics and diagnosis. Hydrol. Process. 30, 2899–2914. https://doi.org/10.1002/hyp.10905.
Pomeroy, J.W., Jones, H.G., Tranter, M., Lilbæk, G.R.O., 2005. Hydrochemical processes in snow-covered basins. Encycl. Hydrol. Sci. 1–14. https://doi.org/10.1002/0470848944.
Pomeroy, J.W., Marsh, P., Lesack, L., 1993. Relocation of major ions in snow along the tundra-taiga ecotone. Hydrol. Res. 24,
Pomeroy, J.W., Toth, B., Granger, R.J., Hedstrom, N.R., Essery, R.L.H., 2003. Variation in surface energetics during snowmelt in a subarctic mountain catchment. J. Hydrometeorol. 4, 702–719. https://doi.org/10.1175/1525-7541(2003)004<0702:VISEDS>2.0.CO;2.
Rasouli, K., Pomeroy, J.W., Janowicz, J.R., Williams, T.J., Carey, S.K., 2018. A long-term hydrometeorological dataset (1993–2014) of a northern mountain basin: Wolf Creek Research Basin, Yukon Territory, Canada. Earth Syst. Sci. Data Discuss. 1–22. https://doi.org/10.5194/essd-2018-118.
Rössler, O., Froidevaux, P., Börst, U., Rickli, R., Martius, O., Weingartner, R., 2014. Retrospective analysis of a nonforecasted rain-on-snow flood in the Alps - a matter of model limitations or unpredictable nature? Hydrol. Earth Syst. Sci. 18, 2265–2285. https://doi.org/10.5194/hess-18-2265-2014.
Scavia, D., David Allan, J., Arend, K.K., Bartell, S., Beletsky, D., Bosch, N.S., Brandt, S.B., Briland, R.D., Daloğlu, I., DePinto, J.V., Dolan, D.M., Evans, M.A., Farmer, T.M., Goto, D., Han, H., Höök, T.O., Knight, R., Ludsin, S.A., Mason, D., Michalak, A.M., Peter Richards, R., Roberts, J.J., Rucinski, D.K., Rutherford, E., Schwab, D.J., Sesterhenn, T.M., Zhang, H., Zhou, Y., 2014. Assessing and addressing the re-eutrophication of Lake Erie: central basin hypoxia. J. Great Lakes Res. 40, 226–246. https://doi.org/10.1016/J.JGLR.2014.02.004.
Selker, J., Leclerq, P., Parlange, J., Steenhuis, T., 1992. Fingered flow in two dimensions. 1. Measurement of matric potential. Water Resour. Res. 28, 2513–2521. https://doi.org/10.1029/92WR00963.
Shiozawa, S., Fujimaki, H., 2004. Unexpected water content profiles under flux-limited one-dimensional downward infiltration in initially dry granular media. Water Resour. Res. 40, W07404. https://doi.org/10.1029/2003WR002197.
Stein, J., Jones, H., Roberge, J., Sochanska, W., 1986. The prediction of both runoff quality and quantity by the use of an integrated snowmelt model. IAHS-AISH publ. 347–358.
Taylor, S., Feng, X., Klaue, B., Albert, M., Kirchner, J., 1998. Using rare earth elements as chemical tracers in snow studies.. 55th Eastern Snow Conference. pp. 13–20.
Tonnessen, K.A., 1991. The Emerald Lake Watershed Study: introduction and site description. Water Resour. Res. 27, 1537–1539. https://doi.org/10.1029/91WR00587.
Tranter, M., 1991. Controls on the Composition of Snowmelt. Seasonal Snowpacks. NATO ASI Series vol. 28. Springer Berlin Heidelberg, Berlin, Heidelberg, pp. 241–271.
Tranter, M., Abrahams, P.W., Blackwood, I., Davies, T.D., Brimblecombe, P., Thompson, I.P., Vincent, C.E., 1987. Changes in streamwater chemistry during snowmelt. Seasonal Snowcovers: Physics, Chemistry, Hydrology. Springer Netherlands, Dordrecht, pp. 575–597.
Vincent, L.A., Zhang, X., Brown, R.D., Feng, Y., Mekis, E., Milewska, E.J., Wan, H., Wang, X.L., Vincent, L.A., Zhang, X., Brown, R.D., Feng, Y., Mekis, E., Milewska, E.J., Wan, H., Wang, X.L., 2015. Observed trends in Canada's climate and influence of low-frequency variability modes. J. Clim. 28, 4545–4560. https://doi.org/10.1175/JCLI-D-14-00697.1.
Wakahama, G., 1963. The infiltration of melt water into snow cover. 1. Low Temp. Sci. Ser. A 21, 45–74. (in Japanese, with English Abstr.).
Waldner, P.A., Schneebeli, M., Schultze-Zimmermann, U., Flühler, H., 2004. Effect of snow structure on water flow and solute transport. Hydrol. Process. 18, 1271–1290. https://doi.org/10.1002/hyp.1401.
Wang, Z., Feyen, J., Ritsema, C.J., 1998. Susceptibility and predictability of conditions for preferential flow. Water Resour. Res. 34, 2169–2182. https://doi.org/10.1029/98WR01761.
Wang, Z., Jury, W.A., Tuli, A., Kim, D.-J., 2004. Unstable flow during redistribution. Vadose Zone J. 3, 549. https://doi.org/10.2136/vzj2004.0549.
Wigington, P., Davies, T., Tranter, M., Eshleman, K., 1990. Acidic deposition: state of science and technology.Report 12. Episodid acidification of surface waters due to acidic deposition. Final report. United States. Technical Report.
Williams, A.P., Seager, R., Abatzoglou, J.T., Cook, B.I., Smerdon, J.E., Cook, E.R., 2015. Contribution of anthropogenic warming to California drought during 2012–2014. Geophys. Res. Lett. 42, 6819–6828. https://doi.org/10.1002/2015GL064924.